

Highly Significant Responses to Anthropogenic Forcings of the Midlatitude Jet in the Southern Hemisphere

ABRAHAM SOLOMON AND L. M. POLVANI

Department of Applied Physics and Applied Mathematics, Columbia University, New York, New York

(Manuscript received 30 December 2015, in final form 18 March 2016)

ABSTRACT

It has been suggested that changes in the atmospheric circulation caused by anthropogenic forcings are highly uncertain, owing to the large natural variability intrinsic to the system. Here, to assess the statistical significance of such changes for the midlatitude, large-scale atmospheric circulation of the Southern Hemisphere, a new 40-member ensemble of integrations, from 1920 to 2080, of the Community Earth System Model, version 5, is analyzed together with a companion 1800-yr-long preindustrial control integration of the same fully coupled model. For simplicity, only the latitudinal position and the strength of the zonal-mean eddy-driven jet are considered. Given the large year-to-year variability of these jet properties, this paper focuses on their decadal averages, which reflect the more slowly varying climate state. The analysis herein reveals that the forced response in such decadal averages easily emerges from the natural variability, with only a few model integrations typically needed to establish statistical significance. In particular, a forced summertime poleward shift of the jet in the latter part of the twentieth century and a strengthening of the jet during the twenty-first century in all seasons of the year are found. Contrasting these with changes in the southern annular mode, this confirms earlier studies demonstrating that such a mode is unable to distinguish different structural changes in the midlatitude jet.

1. Introduction

Assessing uncertainties in modeled projections of climate change is a task of obvious practical importance. Broadly speaking such uncertainties fall into three categories (see, e.g., [Hawkins and Sutton 2009](#)): those due to our inability to know the future external forcings, those related to flaws in the climate models, and those caused by the intrinsic natural variability of the climate system itself. In many ways, the third of these is the most fundamental: even if we knew the forcings exactly and had perfect models, the predictability of the climate system could be very limited if natural variability happened to be sufficiently large—hence the need to quantify such variability.

That was the goal of the pioneering study of [Deser et al. \(2012, hereafter D12\)](#), which tried to assess the emergence of forced signals in the climate system over the period 2005–60. For that period, using an ensemble

of 40 integrations of the Community Climate System Model, version 3 (CCSM3), [D12](#) concluded that future changes in the atmospheric circulation are considerably less robust than changes in surface temperature (and precipitation). Relatively large uncertainties in atmospheric circulation changes, when compared with thermodynamic/radiative changes (especially on regional scales), were also highlighted by [Shepherd \(2014\)](#) in a recent review.

Here we take a different approach to assessing the significance of changes in the atmospheric circulation. Instead of considering surface pressure alone (as in [D12](#)), we study the gross properties (latitude and strength) of the eddy-driven jet in the Southern Hemisphere (SH), where zonal averaging yields a meaningful approximation of the midlatitude circulation. We also broaden the horizon by considering changes from the preindustrial period to the present and into the future, as well as from the present to the future. With this approach, more focused on large-scale properties of the midlatitude jet, we find that changes in the strength and latitude of the SH jet are highly significant in our model, with only a few runs needed to detect changes across different periods.

Corresponding author address: Abraham Solomon, S.W. Mudd Room 200, Columbia University, 500 West 120th Street, New York, NY 10027.
E-mail: as4638@columbia.edu

2. Methods

The data used here consist of monthly-mean, zonal-mean zonal wind and surface pressure from the new Community Earth System Model Large Ensemble Project (CESM-LE), documented by Kay et al. (2015). We analyze 40 coupled integrations from CESM-LE for 1920–2080, with historical forcings prior to 2005 and RCP8.5 scenario forcings afterward. The 40 integrations differ only in their atmospheric initial condition: hence, the ensemble spread reflects the natural variability of the climate system. We also analyze a single, 1800-yr-long, preindustrial (PI) control integration of the same model (with forcings at the year 1850) to establish both the state of the preindustrial climate and its natural variability.

Two key properties of the midlatitude jet are considered: its latitude L and its strength S , here calculated as in Barnes and Polvani (2013), using a quadratic fit to the zonal-mean wind averaged from 700 to 900 hPa. In CESM-LE, the annual-mean values of L and S for the historical period are -51.6° and 14.1 m s^{-1} , respectively; these values compare better with MERRA than most models in phase 5 of the Coupled Model Intercomparison Project (CMIP5; Barnes and Polvani 2013). These two metrics are compared to the southern annual mode (SAM), here calculated as the difference between zonal-mean surface pressure at 40° and 65°S (Gong and Wang 1999). We demonstrate that the SAM response reflects changes in both L and S , making the SAM response difficult to interpret in terms of structural jet changes.

Our statistical analysis is based on first computing decadal averages of the relevant variable. For clarity, decades are designated by their middle year, so that 2075 stands for the decade 2071–80, and 2000 stands for the decade 1996–2005. Let X be the decadal average for any of the three jet variables of interest (L , S , and SAM). Typically, we need to compare two distributions of X [e.g., one distribution from the PI control and another from the large ensemble (LE) at a particular decade]. Each distribution has a mean (\bar{X}_{LE} and \bar{X}_{PI}), a standard deviation (σ_{LE} and σ_{PI}), and a sample size ($N_{\text{LE}} = 40$ and $N_{\text{PI}} = 180$, since we can construct 180 nonoverlapping decadal means from the 1800-yr-long PI control run).

The hypothesis being tested is that the two distributions are different, in which case the variable in a given decade can be said to have significantly changed from the PI control state. For this, the relevant t statistic is the quantity

$$T = \frac{\bar{X}_{\text{PI}} - \bar{X}_{\text{LE}}}{\sqrt{\frac{\sigma_{\text{PI}}^2}{N_{\text{PI}}} + \frac{\sigma_{\text{LE}}^2}{N_{\text{LE}}}}}. \quad (1)$$

We have 95% confidence that the two distributions are different when $|T| > 2$. Conversely, one can ask: What is the minimum number of runs N_{min} needed to detect a change from the PI control in a given decade? To find N_{min} one simply sets $T = 2$ in the above equation and solves for N_{LE} . Note that this method requires knowledge of the population standard deviation (i.e., σ_{LE}) which we estimate from the full 40-member ensemble, but alternatively could have been inferred from the PI control if such a large ensemble were not available.

Our statistical analysis follows directly from the one described in Sardeshmukh et al. (2000) and D12. However, note that D12 did not have a long coupled PI control run at their disposal, so they simply tested whether the distributions across their 40 members were different between the first decade and any subsequent decade: in that case Eq. (1) yields $N_{\text{min}} = 8/(dX/\sigma)^2$, after one sets $\sigma \equiv \sigma_{\text{LE}} = \sigma_{\text{PI}}$, $N \equiv N_{\text{LE}} = N_{\text{PI}}$, and $T = 2$; the quantity dX is the difference of the ensemble means of the variable of interest between the first decade and another decade.

3. Results

We begin by presenting the full seasonal cycles of the southern annual mode, the jet latitude, and jet strength in Fig. 1. In each panel, three curves are plotted, representing three distinct periods: the PI control, the 2000 decade, and the 2075 decade, shown in black, blue, and red, respectively. These three periods, referred to as the past, the present, and the future, were chosen keeping in mind the evolution of stratospheric ozone and greenhouse gases (GHGs), the key forcings¹ of the midlatitude circulation of the SH. Note how each curve in Fig. 1 is surrounded by a confidence interval of width $2\sigma/\sqrt{N}$ (calculated with the respective standard deviation and sample size). When the shaded regions do not overlap, one can immediately deduce that the curves are significantly different at the 95% confidence level.

As the SAM is the most popular metric of the SH midlatitude circulation, we start by discussing the seasonal evolution of the SAM in our model. First, contrast the black and red lines in Fig. 1a: it is clear that in decade 2075 the SAM has significantly increased from its PI control value in every month of the year. The largest seasonal changes occur in December–February (DJF)

¹ Recall that the formation of the ozone hole has acted in concert with GHG forcing in the recent past, but the recovery of the ozone hole in coming decades is projected to cancel much of the DJF seasonal trend due to greenhouse gases (Shindell and Schmidt 2004; Polvani et al. 2011).

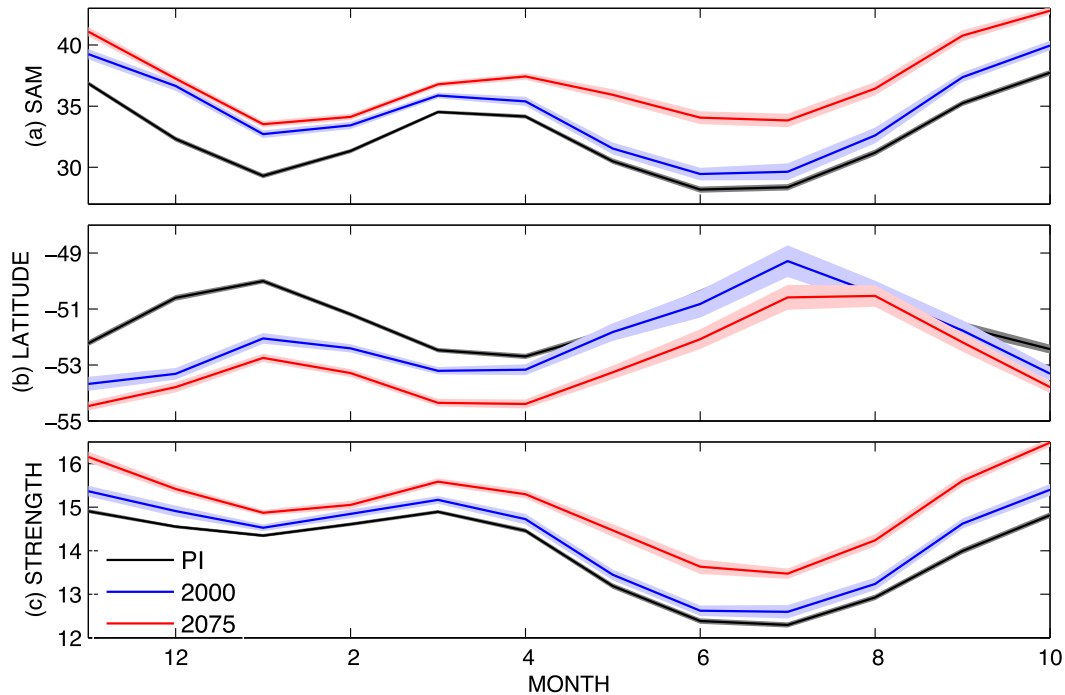


FIG. 1. Monthly-mean values of (top) SAM (hPa), (middle) jet latitude (i.e., L ; $^{\circ}$), and (bottom) jet strength (i.e., S ; m s^{-1}) are plotted for the PI control (black) as well as the ensemble means for decades 2000 (blue) and 2075 (red). The shaded regions surrounding each curve provide the 95% confidence interval for a two-sided t test, given by $2\sigma/\sqrt{N}$ calculated with the respective standard deviations and sample sizes.

and June–August (JJA), so we will focus on these two seasons in subsequent figures. Second, consider the blue line in Fig. 1a: this line shows the present values. Note that in DJF most of the increase in the SAM occurs prior to 2000, with little change afterward (blue and red are close together); in contrast, in JJA there has been little change prior to 2000 (blue and black are close), but a large increase will occur in the twenty-first century. The difference in timing for these two seasonal changes indicates that they are likely driven by different forcings. Even more importantly, we next show that these two SAM trends correspond, in fact, to different changes in the physical properties of the jet.

In terms of the jet latitude, Fig. 1b shows that the jet has shifted poleward significantly during the twentieth century, by nearly 2° in DJF but with basically no shift in JJA. As for the jet strength, Fig. 1c reveals only small changes at present (in all months), but also shows a large and significant increase in JJA in the future (separation of red and blue). These considerations make it clear that SAM changes in JJA are mostly related to changes in S , whereas in DJF they are related to changes in L . The SAM metric, in other words, is confounding different jet properties.

To more fully appreciate the emergence of forced trends in the SH midlatitude circulation in our CESM-LE

runs, we now examine histograms and time series of SAM, L , and S , starting with DJF. For each of these metrics, in Fig. 2 (left) we have plotted histograms of the PDFs for three periods: the past (PI control) in gray, the present (2000) in blue, and the future (2075) in red. Figure 2 (right) shows the time series for each metric: the ensemble mean (in thick black) reveals the forced response, together with 40 individual members of the ensemble (in thin gray). On these panels we superimpose, in green, the values of N_{\min} as defined in Eq. (1).

Figure 2 (top) shows that in DJF the SAM increases by 4 hPa between the past and the future, so that by 2075 SAM changes cannot be explained by natural variability (see how the PDF of the SAM at 2075 does not overlap the PDF of the control). More interesting is the fact that forced SAM changes with respect to the past emerge very early: N_{\min} dips below 3 by 1980, and after 2000 a single member is enough to establish a clear forced response [contrast the blue and gray PDFs in Fig. 2 (top left)]. This may appear surprising, but recall that the quantities we are considering are decadal (not annual) means: the SAM has a huge year-to-year variability, so it makes little sense to use individual years to detect climate changes.

Comparing Figs. 2 (top) and (middle), one can see that the time series of L in DJF closely mirrors that of

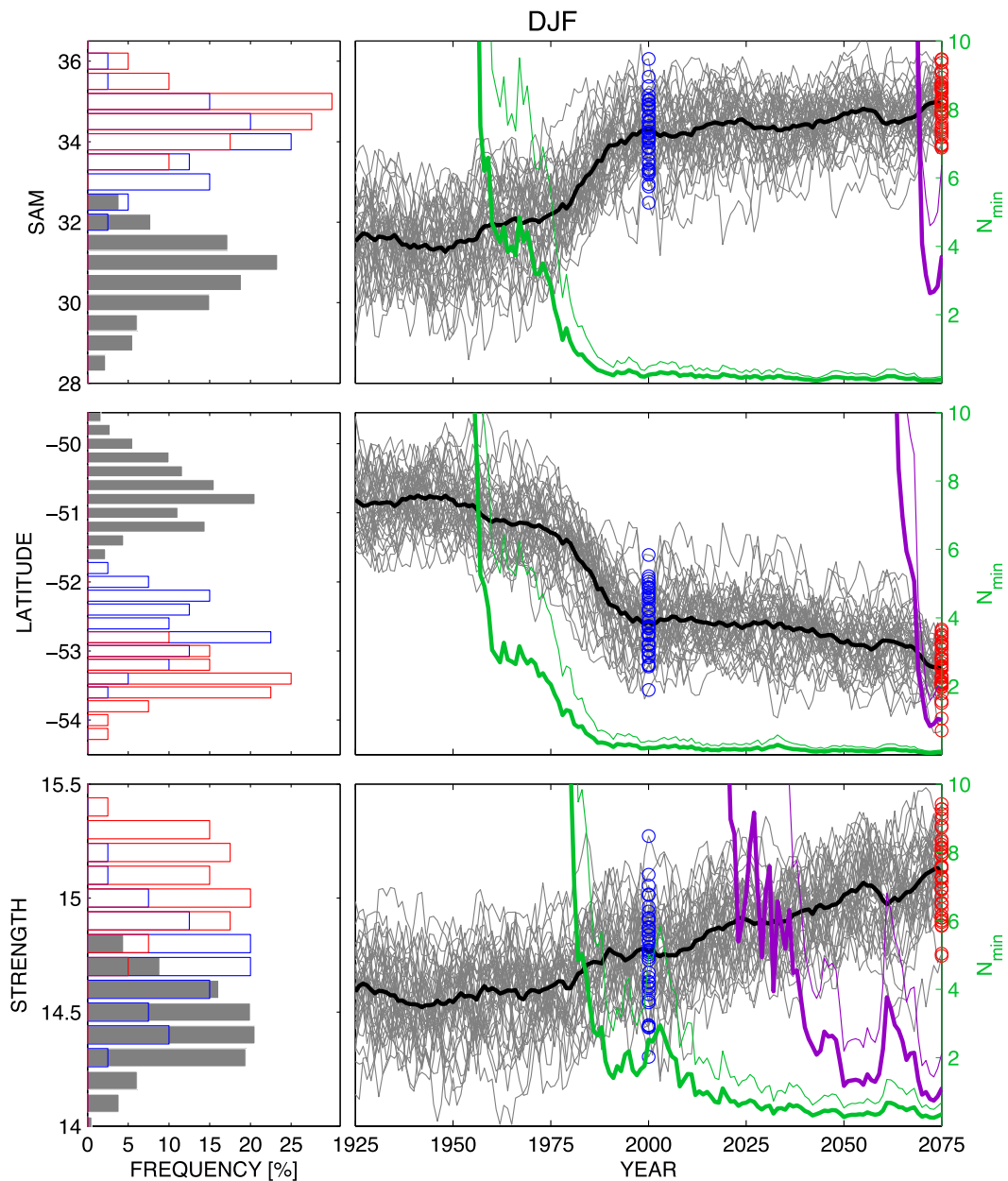


FIG. 2. (left) Histograms of (top) SAM, (middle) L , and (bottom) S constructed from the 180 independent decades of the PI control (gray) and 40 ensemble members for decades 2000 (blue) and 2075 (red). The bin sizes for SAM, L , and S are 0.5 hPa, 0.2° , and 0.1 m s^{-1} , respectively. (right) Time series of DJF decadal-mean values of each variable (running 10-yr average), with the ensemble mean (thick black) and 40 individual ensemble members (thin gray). The thick green curve shows N_{\min} calculated from Eq. (1) for changes from the PI control. The thin green curve shows the approximate value $N_{\min} \approx 8/(dX/\sigma)^2$ used in D12. The purple curves are values of N_{\min} calculated for changes from the decade 2000 (thick and thin defined just as the green curves). The overlaid blue and red circles show the ensemble member values included in the corresponding histograms.

the SAM, with a major poleward jet shift just as SAM increases rapidly from 1970 to 2000, and with small change afterward. The absence of a comparably large poleward shift in JJA over the same period [see Fig. 3 (middle left)] clearly points to the formation of the

ozone hole as the cause for that dramatic shift of the jet in the late twentieth century in our model. In JJA, we find only a weak, but continuous, poleward jet shift, presumably accompanying GHG increases; however, that small JJA shift does not emerge until 2075.

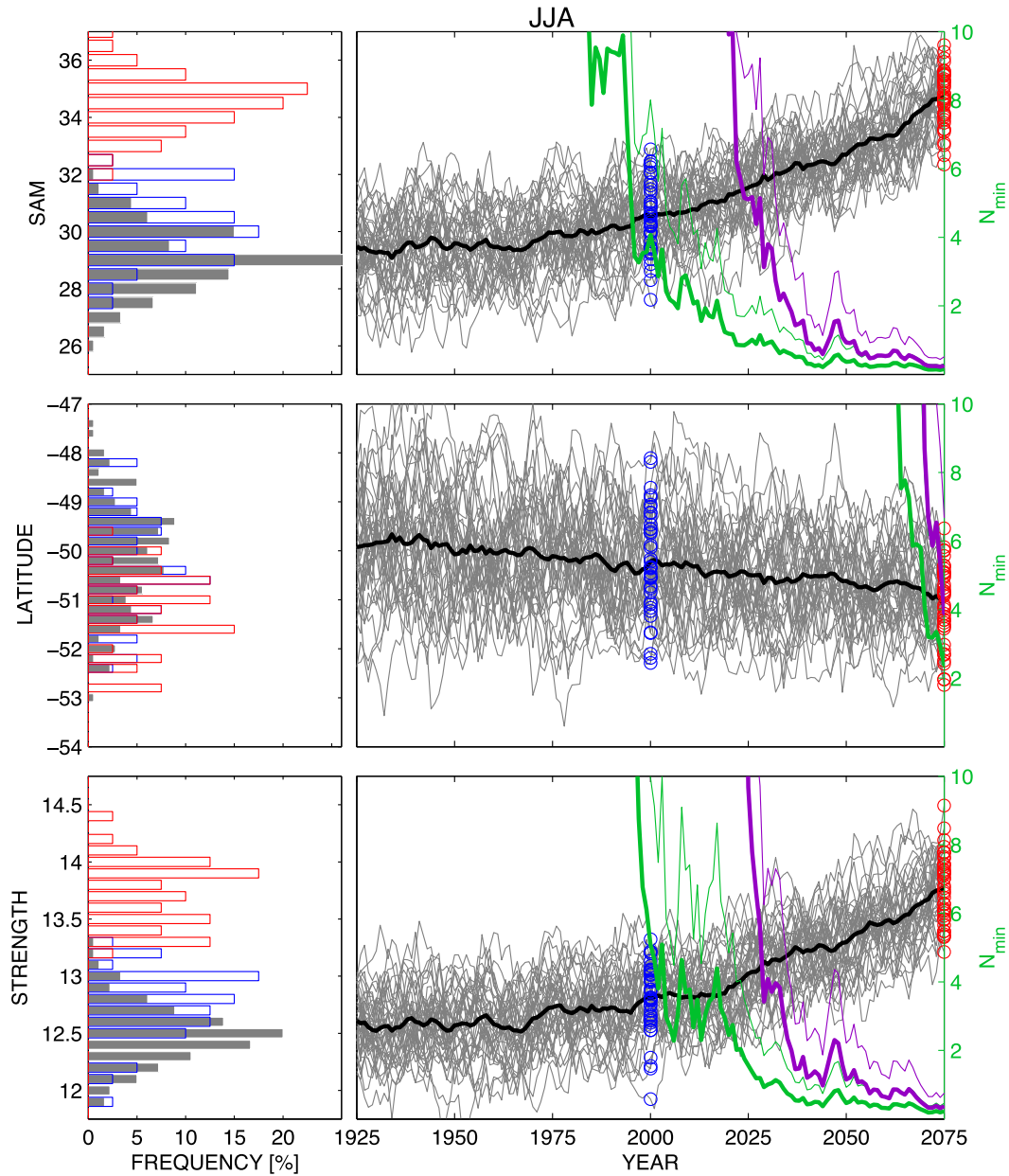


FIG. 3. As in Fig. 2, but for JJA.

As for jet strength, Fig. 2 (bottom) also clearly shows significant forced changes. However, unlike jet latitude, the largest changes in S will happen in the future, as was already noted from Fig. 1. Interestingly, significant DJF jet strengthening actually emerges before 2000 in our model (with $N_{\min} < 2$ after 2010). Note also that, unlike the jet shift, the future strengthening of the jet is even more apparent in JJA (see Fig. 3), clearly pointing to GHG as the underlying forcing agent.

Our analysis up to this point has been limited to zonally averaged quantities: this leaves open the possibility that

important regional changes may be poorly represented by the zonal-mean fields. To address that, we conclude by examining maps of surface pressure p_s and zonal wind U changes, shown in Fig. 4; changes are in color, and the PI climatology in black contours. Figures 4a and 4b show that significant large-scale changes have emerged by 2000 in DJF, and consist of an increase of the pressure gradient (and thus the SAM) associated with a poleward shift of the jet at all longitudes. Comparing Figs. 4a and 4e, one sees that the changes in DJF will further increase over the course of this

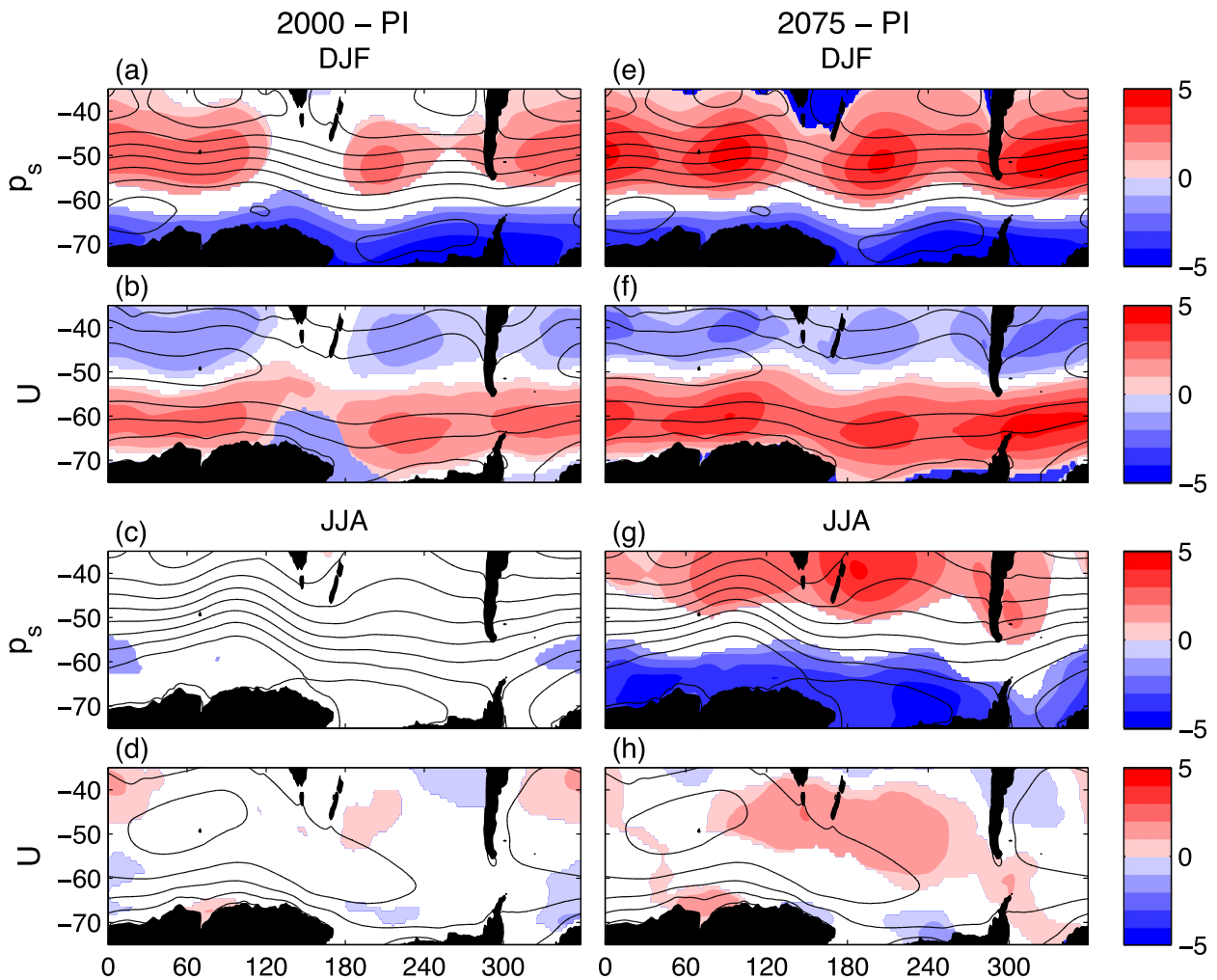


FIG. 4. Changes in p_s (hPa) and U (m s^{-1}) between the PI control and the decades (left) 2000 and (right) 2075 during (a),(b),(e),(f) DJF and (c),(d),(g),(h) JJA. Changes are shown in color only where they are statistically significant at the 95% confidence level. The PI control climatology is overlaid in black contours, with contour intervals of 5 hPa and 5 m s^{-1} , respectively.

century, becoming significant at nearly every location by 2075.

In contrast, for JJA (Figs. 4d,h) one sees little change by 2000 (Fig. 4d), but significant forced changes by 2075 (Fig. 4h) at most longitudes. The 2075–PI changes in U (Fig. 4h) are mostly positive, exceeding 1 m s^{-1} across a broad region, which corresponds to increase in zonal-mean jet strength (Fig. 3, bottom); however, these future changes are far from zonally symmetric. Finally, observe how future p_s changes in DJF and JJA (Figs. 4e,g) both have a north–south dipolar structure, and therefore both result in SAM increases. It is important to note, however, that the associated changes in U do not look similar (cf. Figs. 4f,h). This demonstrates that changes in the SAM must not be simplistically equated with a latitudinal shift of the jet [as noted, e.g., in Barnes and Hartmann (2010)].

4. Summary and discussion

Using the CESM Large Ensemble Project, we have demonstrated that decadal-mean responses of the SH circulation far exceed the natural variability, and are significant with very few members. In DJF a forced poleward shift of the jet has emerged during the twentieth century, and a strengthening of the jet is projected in the twenty-first century (in all months, but with the largest change in JJA). Table 1 summarizes our findings, giving values of N_{\min} for DJF and JJA over several periods: the key point is that all significant changes need only a small number of model runs.

Our results might appear at odds with those of D12, who stressed that thermodynamic changes can be detected with many fewer ensemble members than changes in atmospheric circulation. We can think of several reasons

TABLE 1. Values of N_{\min} computed from Eq. (1) of the SAM, jet latitude (i.e., L), and jet strength (i.e., S) for selected DJF and JJA periods. The first four columns show N_{\min} relative to the PI control for the 2000 and 2075 decades, respectively. The fifth and sixth columns show N_{\min} for changes between the decades 2000 and 2075, by comparing the distributions of the 40 ensemble members, for comparison with D12. Dashes indicate that $N_{\min} > 40$ (i.e., that the changes are not statistically significant).

	2000–PI		2075–PI		2075–2000	
	DJF	JJA	DJF	JJA	DJF	JJA
SAM	1	5	1	1	4	1
L	1	—	1	3	2	4
S	3	6	1	1	2	1

for the discrepancy. First, we have here focused on the gross properties of the jet, including its latitude and strength, rather than focusing on p_s as the primary metric for the circulation. Second, we have explored longer and different² time periods than D12, spanning the eras of ozone depletion as well as recovery. Third, we have taken advantage of a long, coupled PI control, which was not available to D12. This reduces N_{\min} by up to a factor of 2 compared with the estimate in D12, as seen by comparing the thin and thick colored time series in Figs. 2 and 3. Finally, our study has focused on PDFs of decadal averages of the key metrics, not PDFs of trends of those same metrics across specific decades.

Beyond the D12 study, our main findings are supported by a number of recent papers, who have examined modeled trends and natural variability in the SH atmospheric circulation: Swart and Fyfe (2012), Barnes and Polvani (2013), Bracegirdle et al. (2013), and Vallis et al. (2015) have reported a significant poleward shift and strengthening of the Southern Hemisphere jet in the models participating in CMIP5. However, examining the same CMIP5 models for the period 1979–2005 while taking into account the natural variability of each model (computed from corresponding century-long PI control integrations), Thomas et al. (2015) concluded that the modeled trends over that recent period cannot be distinguished from natural variability in the models. That conclusion is based specifically on 25-yr linear trends for that one period, whereas our conclusions are based upon the

distribution of decadal means, so the two results do not contradict one another, but rather underscore the challenge of establishing the significance of trends over relatively short periods. Finally, our analysis confirms the recent finding of Swart et al. (2015), who have also noted how structural changes of the eddy-driven midlatitude jet are difficult to infer from SAM changes alone.

Acknowledgments. This work is funded by a Frontiers in Earth System Dynamics (FESD) grant from the National Science Foundation. The computations were carried out with high-performance computing support provided by NCAR’s Computational and Information Systems Laboratory, which is sponsored by the National Science Foundation. The data produced for and analyzed in this paper are archived on the High Performance Storage System (HPSS) at NCAR, and can be provided upon request.

REFERENCES

- Barnes, E. A., and D. L. Hartmann, 2010: Dynamical feedbacks of the southern annular mode in winter and summer. *J. Atmos. Sci.*, **67**, 2320–2330, doi:10.1175/2010JAS3385.1.
- , and L. Polvani, 2013: Response of the midlatitude jets, and of their variability, to increased greenhouse gases in the CMIP5 models. *J. Climate*, **26**, 7117–7135, doi:10.1175/JCLI-D-12-00536.1.
- Bracegirdle, T. J., E. Shuckburgh, J.-B. Sallee, Z. Wang, A. J. S. Meijers, N. Bruneau, T. Phillips, and L. J. Wilcox, 2013: Assessment of surface winds over the Atlantic, Indian, and Pacific Ocean sectors of the Southern Ocean in CMIP5 models: Historical bias, forcing response, and state dependence. *J. Geophys. Res. Atmos.*, **118**, 547–562, doi:10.1002/jgrd.50153.
- Deser, C., A. Phillips, V. Bourdette, and H. Teng, 2012: Uncertainty in climate change projections: The role of internal variability. *Climate Dyn.*, **38**, 527–546, doi:10.1007/s00382-010-0977-x.
- Gong, D., and S. Wang, 1999: Definition of Antarctic oscillation index. *Geophys. Res. Lett.*, **26**, 459–462, doi:10.1029/1999GL900003.
- Hawkins, E., and R. Sutton, 2009: The potential to narrow uncertainty in regional climate predictions. *Bull. Amer. Meteor. Soc.*, **90**, 1095–1107, doi:10.1175/2009BAMS2607.1.
- Kay, J., and Coauthors, 2015: The Community Earth System Model (CESM) Large Ensemble Project: A community resource for studying climate change in the presence of internal climate variability. *Bull. Amer. Meteor. Soc.*, **96**, 1333–1349, doi:10.1175/BAMS-D-13-00255.1.
- Polvani, L. M., M. Previdi, and C. Deser, 2011: Large cancellation, due to ozone recovery, of future Southern Hemisphere atmospheric circulation trends. *Geophys. Res. Lett.*, **38**, L04707, doi:10.1029/2011GL046712.
- Sardeshmukh, P. D., G. P. Compo, and C. Penland, 2000: Changes of probability associated with El Niño. *J. Climate*, **13**, 4268–4286, doi:10.1175/1520-0442(2000)013<4268:COPAWE>2.0.CO;2.

² For a more direct comparison with D12, in Figs. 2 and 3 we have plotted, in purple, the values of N_{\min} for changes relative to the 2000 decade. Confirming the findings of D12, we see little significant SAM (and jet latitude) response in DJF prior to 2060. Note, however, that the increase in jet strength is significant, for both DJF and JJA, by midcentury (relative to 2000): this was not reported in D12, likely due to their reliance on p_s .

- Shepherd, T. G., 2014: Atmospheric circulation as a source of uncertainty in climate change projections. *Nat. Geosci.*, **7**, 703–708, doi:[10.1038/ngeo2253](https://doi.org/10.1038/ngeo2253).
- Shindell, D. T., and G. A. Schmidt, 2004: Southern Hemisphere climate response to ozone changes and greenhouse gas increases. *Geophys. Res. Lett.*, **31**, L18209, doi:[10.1029/2004GL020724](https://doi.org/10.1029/2004GL020724).
- Swart, N., and J. Fyfe, 2012: Observed and simulated changes in the Southern Hemisphere surface westerly wind-stress. *Geophys. Res. Lett.*, **39**, L16711, doi:[10.1029/2012GL052810](https://doi.org/10.1029/2012GL052810).
- , ——, N. Gillett, and G. J. Marshall, 2015: Comparing trends in the southern annular mode and surface westerly jet. *J. Climate*, **28**, 8840–8859, doi:[10.1175/JCLI-D-15-0334.1](https://doi.org/10.1175/JCLI-D-15-0334.1).
- Thomas, J. L., D. W. Waugh, and A. Gnanadesikan, 2015: Southern Hemisphere extratropical circulation: Recent trends and natural variability. *Geophys. Res. Lett.*, **42**, 5508–5515, doi:[10.1002/2015GL064521](https://doi.org/10.1002/2015GL064521).
- Vallis, G. K., P. Zurita-Gotor, C. Cairns, and J. Kidston, 2015: Response of the large-scale structure of the atmosphere to global warming. *Quart. J. Roy. Meteor. Soc.*, **141**, 1479–1501, doi:[10.1002/qj.2456](https://doi.org/10.1002/qj.2456).